A Numerical Investigation of the Efficiency with which Simple Columnar Ice Crystals Collide with Supercooled Water Drops

R. J. SCHLAMP AND H. R. PRUPPACHER

Department of Meteorology, University of California, Los Angeles 90024

A. E. HAMIELEC

Department of Chemical Engineering, McMaster University, Hamilton, Canada

(Manuscript received 4 June 1975, in revised form 3 September 1975)

ABSTRACT

The Navier-Stokes equation of motion for two-dimensional, viscous, steady-state incompressible flow past an infinitely long circular cylinder was solved by numerical techniques for Reynolds numbers between 0.1 and 50. From the streamfunction and vorticity fields the pressure at the cylinder surface, the pressure drag, and the frictional drag were computed, and from the latter two the total drag on the cylinder was derived. The values found for the drag compared well with the best theoretical and experimental values reported in literature, suggesting that our flow fields were sufficiently accurate. These flow fields were used to determine the hydrodynamic interaction between simple columnar ice crystals idealized as circular cylinders of finite length L', of radius a_L', and of Reynolds number $N_{Re,L}$ ($67.1 \leqslant L' \leqslant 2440$ μm; $23.5 \leqslant a_L' \leqslant 146.4$ μm; $0.2 \leqslant N_{Re,L} \leqslant 20$) and spherical water drops of radius a_S' varying between 2 and 134 μm. The flow fields used to describe the flow past drops were numerically computed by a method analogous to that given by LeClair *et al.* (1970). For atmospheric conditions of −8°C and 800 mb numerical methods were used to determine the trajectory of the drops relative to the cylinder by means of a semi-empirically modified version of the "superposition" model. The model was semi-empirical in that the flow fields used were those determined theoretically by us, while the drag on the columnar crystals was that determined by Jayaweera and Cottis (1969) and by Kajikawa (1971), and the dimensional relationships between the diameter and length of the columnar crystal were those given by the observational relations of Auer and Veal (1970). From the trajectories of the water drops relative to the columnar ice crystals collision efficiencies were computed. Our computations predict that riming on a columnar ice crystal will not commence until the crystal has a diameter which is larger than about 50 μm. This result is in good agreement with field observations reported in literature.

1. Introduction

The riming process during which ice crystals collide with supercooled water drops is of considerable importance to the formation of precipitation in atmospheric clouds in that it is the process by which ice crystals efficiently grow to graupel particles and hailstones. Pitter and Pruppacher (1974) pointed out that in most earlier studies on this process it was assumed that the collision efficiency of ice crystals could be approximated by those of spheres of the same size. However, numerous investigations reported in literature [for a summary see Mason (1971)] have shown that the basic shape of an ice crystal growing by diffusion in water vapor is that of a hexagonal prism. Depending upon the temperature and the supersaturation of water vapor, the ice prism either grows predominantly along the crystallographic *c* axis (columnar ice crystals) or along the crystallographic *a* axis (platelike and dendritic crystals). In recognition of this fact, some attempts have recently been made to obtain collision efficiencies for bodies of ice crystal shape. Thus, Ono (1969) and Wilkins and Auer (1970) suggested the use of collision efficiencies which were derived by Ranz and Wong (1952) on the basis of inviscid flow past disks. However, since single ice crystals in atmospheric clouds have Reynolds numbers typically less than 100, it is not justified to apply potential flow theory. For hexagonal columns, Ono (1969) derived collision efficiencies based on the results of Davies and Peetz (1956) who determined the efficiency with which spherical particles collide with an infinitely long cylinder of Reynolds number 0.2, assuming creeping flow around the cylinder, and of Reynolds number 10 using the numerical flow field of Thom (1933). As shown by Pruppacher *et al.* (1970), creeping flow is not a good approximation to viscous flow past bodies of Reynolds numbers larger than 0.1, and the numerical computations of Thom do not accurately represent viscous flow past a cylinder at Reynolds number 10.

Realizing these difficiencies, Pitter *et al.* (1973) solved the Navier-Stokes equation of motion for viscous flow

past thin, oblate spheroids of Reynolds numbers between 0.1 and 100. Based on the experimental evidence that the hydrodynamic behavior of a simple hexagonal plate may well be approximated by that of a circular disk or of a thin oblate spheroid, Pitter and Pruppacher (1974) used these flow fields to compute the efficiency with which spherical water drops of radii up to 53 μm collide with simple hexagonal plate-like ice crystals of radii 147 to 404 μm. In good agreement with observations in natural clouds, Pitter and Pruppacher found that riming takes place preferentially along the rim of plate-like ice crystals, and further, that plate-like ice crystals need to grow by diffusion to a radius of about 150 μm before riming will commence.

2. Method of approaching the present problem

Encouraged by the realistic results which we theoretically obtained for the case of plate-like crystals, and motivated by the current need for collision efficiencies for ice crystals of all shapes, we attempted to compute the efficiency with which *columnar shaped* ice crystals collide with supercooled water drops. In order to carry out this attempt we proceeded in three steps. During the first step we solved the Navier-Stokes equation of motion for steady-state, viscous, incompressible flow past *infinitely long circular cylinders* of various Reynolds numbers. During the second step we computed the trajectories of spherical water drops of various sizes interacting with a columnar ice crystal. For carrying out this second step we first assumed that the *velocity field past a circular cylinder of finite length* can be *approximated to sufficient accuracy by the velocity field* we computed *for an infinitely long circular cylinder*. This assumption, in essence, means that the trajectory of a cloud drop in its motion around a circular cylinder of finite length is only negligibly affected by flow components along the cylinder axis and almost completely determined by the flow in a plane perpendicular to the columnar axis. We felt that this assumption is reasonably justified by the observations of Ono (1969), Iwai (1973) and Zikmunda and Vali (1972) who demonstrated that in contrast to plate-like crystals, drops on rimed columnar ice crystals are fairly uniformly distributed (see Fig. 1) over the whole crystal surface suggesting that the columnar ends are not significantly affecting the collection efficiency of ice crystals. We next assumed that a hexagonal columnar ice crystal fluid dynamically behaves as a circular cylindrical ice crystal. The experimental determinations of Jayaweera and Cottis (1969) justify this assumption. On the other hand, we were aware of the fact that the fluid dynamic drag of cylindrical crystals with a diameter to length ratio larger than 1:10 is not represented with sufficient accuracy by the drag of an infinitely long cylinder (Jayaweera and Cottis, 1969). Since this quantity enters into the trajectory calculations, we *did not use the drag which we computed for an infinitely long cylinder but computed the trajectories on the bases of drag force coefficients which were empirically determined* by Jayaweera and Cottis (1969) and by Kajikawa (1971), and on the bases of the columnar length to diameter relationships given by Auer and Veal (1970). During step three of our computational procedure, collision efficiencies were determined from the computed trajectories.

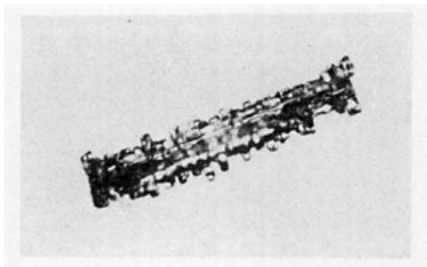

FIG. 1. Rimed columnar crystal (Courtesy of Dr. K. Iwai).

3. Numerical determination of the flow field around an infinitely long circular cylinder

A fair number of studies have been reported in the literature on solving the steady-state Navier-Stokes equation of motion for viscous incompressible flow past an infinitely long circular cylinder (Griffin, 1972; Hamielec and Raal, 1969; Dennis and Shimshoni, 1964; Keller and Takami, 1966; Takami and Keller, 1969; Underwood, 1969; Dennis and Chang, 1970; Nieuwstadt and Keller, 1973). Since in none of these studies are values for the streamfunction listed in a manner which is sufficiently detailed for use in trajectory computations, and since in several previous studies the boundaries in the numerical computations were not kept sufficiently far away from the cylinder surface, it was necessary to compute anew the flow field past infinitely long circular cylinders. The procedure to carry out this task is summarized below.

Considering steady-state viscous flow, normal to an infinitely long circular cylinder, one may treat the problem as two-dimensional, and may describe the flow in terms of the plane polar coordinates r, θ. The Navier-Stokes equation of motion for steady-state, viscous incompressible flow may then be written in nondimensionalized form as

$$\nabla^4\psi = (N_{\mathrm{Re},L}/2r)\left[\frac{\partial\psi}{\partial r}\frac{\partial}{\partial\theta}(\nabla^2\psi) - \frac{\partial\psi}{\partial\theta}\frac{\partial}{\partial r}(\nabla^2\psi)\right], \quad (1)$$

where

$$\left.\begin{aligned} r = r'/a_L' \quad &, \quad \psi = \psi'/V_{\infty,L}'a_L' \\ N_{\mathrm{Re},L} = 2a_L'V_{\infty,L}'/\nu', \quad &\zeta = \zeta' a_L'/V_{\infty,L}' \end{aligned}\right\}, \quad (2)$$

in which primed quantities are dimensional. More conveniently, Eq. (1) may be split into two second-order differential equations by introducing the vorticity.

TABLE 1. Computational parameters used for present numerical computations.

$N_{Re,L}$	0.1	0.2	0.5	0.7	1.0	2.0	5.0	10.0	20.0	30.0	40.0	50.0
Grid size	41×95	41×95	41×95	41×95	41×95	41×95	41×87	61×111	61×101	61×101	61×91	61×91
A	0.075	0.075	0.075	0.075	0.075	0.075	0.075	0.05	0.05	0.05	0.05	0.05
B	4.5°	4.5°	4.5°	4.5°	4.5°	4.5°	4.5°	3°	3°	3°	3°	3°
r_∞	1152.9	1152.9	1152.9	1152.9	1152.9	1152.9	632.7	244.7	148.4	148.4	90.0	90.0

This gives

$$\left.\begin{aligned} &\nabla^2\zeta=(N_{\mathrm{Re},L}/2r)\left(\frac{\partial\psi}{\partial r}\frac{\partial\zeta}{\partial\theta}-\frac{\partial\psi}{\partial\theta}\frac{\partial\zeta}{\partial r}\right)\\ &\text{with}\qquad \zeta=\nabla^2\psi\\ &\text{where}\qquad \nabla^2=\frac{\partial^2}{\partial r^2}+\frac{1}{r}\frac{\partial}{\partial r}+\frac{1}{r^2}\frac{\partial^2}{\partial\theta^2}\end{aligned}\right\}. \tag{3}$$

Near the cylinder surface, a small step size is needed where the streamfunction and the vorticity vary most rapidly. In order to take this requirement into account we followed the customary procedure to set $r=e^z$, which allowed for a constant step size Δz. Eqs. (3) then become

$$\left.\begin{aligned} &\nabla^2\zeta=(N_{\mathrm{Re},L}/2)\left(\frac{\partial\psi}{\partial z}\frac{\partial\zeta}{\partial\theta}-\frac{\partial\psi}{\partial\theta}\frac{\partial\zeta}{\partial z}\right)\\ &\text{with}\qquad \zeta=e^{-2z}\nabla^2\psi\\ &\text{where}\qquad \nabla^2=\frac{\partial^2}{\partial z^2}+\frac{\partial^2}{\partial\theta^2}\end{aligned}\right\}. \tag{4}$$

Eqs. (4) were simultaneously solved for $N_{\mathrm{Re}}=0.1$, 0.2, 0.5, 0.7, 1.0, 2.0, 5.0, 10.0, 20.0, 30.0, 40.0, 50.0 by numerical procedures which essentially followed those used by Woo (1971) subject to the boundary conditions:

Along the axis of symmetry: $\theta=0,\pi,\ \psi=0,\ \zeta=0$

On the cylinder surface: $z=0,\ \psi=0,\ \zeta=\nabla^2\psi,\ \partial\psi/\partial z=0$

On a cylindrical boundary concentric with the cylinder but remote from its surface: $z=z_\infty,\ \psi=e^{z_\infty}\sin\theta,\ \zeta=0$. (5)

The values for the radial step size A, the angular step size B, and the distance r_∞ to the boundary used in our computations are listed in Table 1. The solutions were considered to have converged when the residuals (R)

$$\left.\begin{aligned} \psi^{(R)}(I,J)&=[\psi^{n+1}(I,J)-\psi^n(I,J)]/\psi^{n+1}(I,J)\\ \zeta^{(R)}(I,J)&=[\zeta^{n+1}(I,J)-\zeta^n(I,J)]/\zeta^{n+1}(I,J)\end{aligned}\right\} \tag{6}$$

had a value of less than 10^{-5} at all grid points.

To check the accuracy of our solutions for ψ and ζ, several integral properties of the flow were determined: The pressure distribution around the cylinder

$$k(\theta)=k(\theta=0)+\frac{4}{N_{\mathrm{Re},L}}\int_0^\theta\left(\frac{\partial\zeta}{\partial z}\right)_{z=0}d\theta \tag{7}$$

The frontal stagnation pressure

$$k(\theta=0)=1+\frac{4}{N_{\mathrm{Re},L}}\int_0^{z_\infty}\left(\frac{\partial\zeta}{\partial\theta}\right)_{\theta=0}dz \tag{8}$$

TABLE 2. Comparison of drag force coefficient for an infinite cylinder computed by present numerical method, with values cited in literature.

$N_{Re,L}$	0.1	0.2	0.5	1.0	2.0	5.0	10.0	20.0	30.0	40.0	50.0
Present (theory)	56.72	32.91	16.72	10.38	6.68	3.94	2.77	2.01	1.68	1.50	1.37
Nieuwstadt and Keller (1973) (theory)	—	—	—	10.31	—	—	2.83	2.05	1.73	1.55	—
Griffin (1972) (theory)	—	34.91	17.97	10.88	—	4.01	2.78	2.00	1.68	1.56	—
Dennis and Chang (1970) (theory)	—	—	—	—	—	4.12	2.85	2.05	—	1.52	—
Hamielec and Raal (1969) (theory)	60.33	—	—	10.65	—	—	2.82	—	1.75	—	1.46
Takami and Keller (1969) (theory)	—	—	—	10.28	6.63	—	2.75	2.00	1.72	1.54	1.42
Keller and Takami (1966) (theory)	—	—	—	—	6.64	—	2.74	—	—	—	—
Dennis and Shimshoni (1964) (theory)	56.57	—	17.06	10.37	6.73	—	2.99	2.33	—	1.99	—
Nishioka and Sato (1974) (experiment)	—	—	—	—	—	—	2.79	1.97	1.62	1.49	1.40

The pressure drag coefficient

$$C_{DP}=\int_0^{\pi}[k(\theta)]_{z=0}\cos\theta d\theta \tag{9}$$

The viscous drag coefficient

$$C_{DF}=\frac{4}{N_{\mathrm{Re},L}}\int_0^{\pi}\zeta_{z=0}\sin\theta d\theta \tag{10}$$

In the above $C_D=C_{DP}+C_{DF}$. Eq. (7) was evaluated using the trapezoidal rule while Eqs. (8)–(10) were evaluated using Simpson's rule.

In agreement with the experimental results of Taneda (1956) and Homan (1936) and the most accurate computations reported in literature, our calculated flow fields developed a standing eddy at the downstream end of the cylinder at $N_{\mathrm{Re},L}\approx 6$, growing in length with increasing $N_{\mathrm{Re},L}$ in a manner described by Pruppacher *et al.* (1970). Since most authors reported values for C_D at the same $N_{\mathrm{Re},L}$ it was impractical to make a graphic comparison between the various values of C_D reported in literature. Instead, we decided to make such a comparison in tabular form (Table 2). It is seen from this table that our computed values of C_D are in good agreement with the values for C_D computed by other authors although our values are slightly lower than those of most authors as a result of the fact that our boundaries were somewhat farther removed from the cylinder surface than those of most authors, thus reducing the error due to boundary effects.

4. Numerical determination of the trajectory of spherical drops moving relative to a circular cylindrical ice crystal of finite length

Klett and Davis (1973) have discussed in detail the difficulties associated with the exact determination of collision efficiencies for two interacting spheres falling under the influence of gravity in an otherwise undisturbed fluid. They also discussed the simplifications which can be made in order to solve the collision efficiency problem, and the cost of such simplifications to the physical realism of the problem. In order to model the hydrodynamic interaction of two spheres with as much physical realism as possible, they used an analytical method, based on a modified form of the Oseen equations for the flow field, and simultaneously satisfied the changing boundary conditions at the surfaces of the two spheres during the interaction. While such an analytical treatment would also be highly desirable for the case of hydrodynamic interaction between an ice crystal and a water drop, the complex geometry associated with this interaction presently prohibits it.

We therefore chose the so-called "superposition scheme" which models such interactions though it neglects the close boundary effects since it assumes that each body moves in the stream caused by the fluid motion around the other body in isolation. It has been argued that this method does not give accurate account of the hydrodynamic interaction between two spheres when they are very close to each other, in particular when they have similar sizes. Indeed, a comparison between the collision efficiencies computed by Shafrir and Neiburger (1963) for spheres on the basis of the superposition scheme with those computed by the analytical method of Klett and Davis (1973) and with the experimental results of Woods and Mason (1965) suggests that the objections to this method are valid when the two interacting spheres have similar size. This disagreement manifests itself in that the results of Shafrir and Neiburger suggest that the collision efficiency decreases to zero for all collector drops as the two interacting spheres become similarly sized in contrast to the results of Klett and Davis and the experimental results of Woods and Mason which show that, following a relative minimum, the collision efficiency increases sharply as the two interacting spheres become of similar size, a result which must be attributed to wake effects. However, in later computations, Neiburger (1967) and Shafrir and Gal-Chen (1971), using the same superposition method, arrived at collision efficiencies which, for collector drops larger than 60 μm, were considerably different than those of Shafrir and Neiburger. In closer agreement with experiment the new collision efficiencies sharply increased for the case of two interacting spheres of similar size. This result suggests that, when properly applied, the superposition scheme will reproduce the essential features of two fluid dynamically interacting spheres. This conclusion is particularly supported by the results of Lin and Lee (1975) who, by using the superposition scheme, correctly predict that the collision efficiency of collector drops >20 μm does not decrease to zero but sharply increases as the two interacting spheres become of similar size, and agrees reasonably well with the collision efficiencies computed by Klett and Davis. Encouraged by this result we decided to apply the superposition scheme to the problem of hydrodynamically interacting columnar ice crystals and water drops.

The equations of motion for a cylindrical ice crystal and a spherical drop are

$$m_L'\frac{d\mathbf{V}_L'}{dt'}=m_L'\mathbf{g}_L^{*'}-\mathbf{f}_{D,L}', \tag{11}$$

$$m_S'\frac{d\mathbf{V}_S'}{dt'}=m_S'\mathbf{g}_S^{*'}-\mathbf{f}_{D,S}', \tag{12}$$

with

$$\mathbf{g}_{L,S}^{*'}=[(\rho_{L,S}'-\rho_a')/\rho_{L,S}']\mathbf{g}'. \tag{13}$$

In terms of the superposition scheme used by Shafrir and Neiburger (1963), Eqs. (11) and (12) can be

written as

$$m_L'\frac{d\mathbf{V}_L'}{dt'}=m_L'\mathbf{g}_L^{*\prime}-12L'\mu'\left(\frac{C_{D,L}N_{\mathrm{Re},L}}{24}\right)(\mathbf{V}_L'-\mathbf{U}_S'), \quad (14)$$

$$m_S'\frac{d\mathbf{V}_S'}{dt'}=m_S'\mathbf{g}_S^{*\prime}-6\pi a_S'\mu'\left(\frac{C_{D,S}N_{\mathrm{Re},S}}{24}\right)(\mathbf{V}_S'-\mathbf{U}_L'). \quad (15)$$

Eqs. (14) and (15) were non-dimensionalized by setting

$$\left.\begin{aligned}&\mathbf{V}=\mathbf{V}'/V_{\infty,L}'; \quad t=t'V_{\infty,L}'/a_L';\\ &\qquad\mu=\mu'(a_L')^2/m_L'V_{\infty,L}'; \quad q=\rho_L'/\rho_S'\\ &\mathbf{U}=\mathbf{U}'/V_{\infty,L}'; \quad \mathbf{g}^*=\mathbf{g}^{*\prime}a_L'/(V_{\infty,L}')^2;\\ &\qquad p=a_S'/a_L'; \quad AR=a_L'/L'\end{aligned}\right\}. \quad (16)$$

With these, Eqs. (14) and (15) become

$$\frac{d\mathbf{V}_L}{dt}=\mathbf{g}_L^*-Q_2(\mathbf{V}_L-\mathbf{U}_S), \quad (17)$$

with

$$Q_2=\tfrac{1}{2}(\mu C_{D,L}N_{\mathrm{Re},L}/AR), \quad (18)$$

$$\frac{d\mathbf{V}_S}{dt}=\mathbf{g}_s^*-Q_1(\mathbf{V}_S-\mathbf{U}_L), \quad (19)$$

$$Q_1=(3\pi q\mu/p^2AR)(C_{D,S}N_{\mathrm{Re},S}/16). \quad (20)$$

Setting $d\mathbf{R}/dt=\mathbf{V}$, Eqs. (17) and (19) may be written in component form in a fixed reference frame (Fig. 2) as

$$\left.\begin{aligned}&\frac{dR_{Lx}}{dt}=V_{Lx}; \quad \frac{dV_{Lx}}{dt}=g_L^*-Q_2(V_{Lx}-U_{Sx})\\ &\frac{dR_{Ly}}{dt}=V_{Ly}; \quad \frac{dV_{Ly}}{dt}=-Q_2(V_{Ly}-U_{Sy})\end{aligned}\right\} \quad (21)$$

and

$$\left.\begin{aligned}&\frac{dR_{Sx}}{dt}=V_{Sx}; \quad \frac{dV_{Sx}}{dt}=g_S^*-Q_1(V_{Sx}-U_{Lx})\\ &\frac{dR_{Sy}}{dt}=V_{Sy}; \quad \frac{dV_{Sy}}{dt}=-Q_1(V_{Sy}-U_{Ly})\end{aligned}\right\} \quad (22)$$

Eqs. (21) and (22) determine the trajectory of an interacting drop and ice crystal. In addition, the following relationship, which readily is derived from basic hydrodynamic concepts, was used:

$$C_{D,L}N_{\mathrm{Re},L}=2\pi(a_L')^2(\rho_L'-\rho_a')g'/V_{\infty,L}'\mu'. \quad (23)$$

Multiplying both sides by $N_{\mathrm{Re},L}=2a_L'V_{\infty,L}'\rho_a'/\mu'$ and rearranging terms, one finds

$$a_L'=[C_{D,L}N_{\mathrm{Re},L}^2(\mu')^2/4\pi\rho_a'(\rho_L'-\rho_a')g']^{\frac{1}{3}}. \quad (24)$$

For our computations we chose as environmental conditions an atmosphere with a pressure of 800 mb and with a temperature of −8°C. The dynamic viscosity of the air is then $\mu'=1.677\times10^{-5}$ kg m^{-1} s^{-1} ($=1.677\times10^{-4}$ poise). The bulk density of the columnar ice crystal was chosen as $\rho_L'=0.6\times10^{-3}$ kg m^{-3}, considering that the ice crystal is partially hollow. The bulk density of water was set $\rho_S'=0.99847\times10^{-3}$ kg m^{-3}, and $g'=9.8$ m s^{-2}.

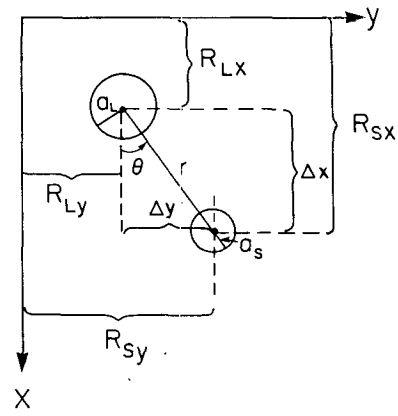

FIG. 2. Schematic of interacting sphere and cylinder in coordinate system used, with $\Delta x=R_{Sx}-R_{Lx}$, $\Delta y=R_{Sy}-R_{Ly}$, $\theta=\tan^{-1}(\Delta y/\Delta x)$, and $r=[(\Delta x)^2+(\Delta y)^2]^{\frac{1}{2}}$.

The quantity Q_2 [Eq. (18)] was determined by the following procedure. Based on the measurements of Jayaweera and Cottis (1969) and of Kajikawa (1971) we plotted a diagram giving $C_{D,L}N_{\mathrm{Re},L}^2$ vs AR for each of the $N_{\mathrm{Re},L}$ for which we had flow fields computed. Choosing an available $N_{\mathrm{Re},L}$ and selecting a value for AR, the corresponding $C_{D,L}N_{\mathrm{Re},L}^2$ was graphically determined. This value was inserted into Eq. (24) and a_L' was computed. Since $AR=a_L'/L'$, the chosen value for AR and the computed value for a_L' determined a corresponding L'. Since Auer and Veal (1970), among others, found that ice crystals in atmospheric clouds only assume certain dimensions which are strictly related to each other, each a_L',L' dimensional pair we computed was checked against Auer and Veal's dimensional relationship for columnar crystals. In case the a_L',L' pair did not agree with the Auer and Veal relationship, a new value for AR was chosen, and the above procedure repeated until there was agreement within Auer and Veal's observational scatter. Having thus found a_L' for a given $N_{\mathrm{Re},L}$ we computed $V_{\infty,L}'$ from

$$V_{\infty,L}'=\mu'N_{\mathrm{Re},L}/2a_L'\rho_a'. \quad (25)$$

With a complete set of corresponding values for $N_{\mathrm{Re},L}$, AR, a_L', $C_{D,L}$ and $V_{\infty,L}'$, Q_2 was computed from Eq. (18) and g_L^* from Eqs. (16) and (13).

The quantity Q_1 [Eq. (20)] was determined by the following procedure. A value for the drop size a_S' was chosen. This allowed us to compute $C_{D,L}N_{\mathrm{Re},S}^2$ from

$$c_{DS}N_{\mathrm{Re},S}^2=\frac{32}{3}[(a_S')^3g'\rho_a'(\rho_s'-\rho_a')/(\mu')^2]. \quad (26)$$

Using the empirical formulas of Beard (1974) which give $C_{D,S}N_{\mathrm{Re},S}^2$ vs $N_{\mathrm{Re},S}$ for spheres, $N_{\mathrm{Re},S}$ and thus

$C_{D,S}N_{\mathrm{Re},S}$ and Q_1 could be determined. Once $N_{\mathrm{Re},S}$ was established $V'_{\infty,S}$ could be found from an equation analogous to Eq. (25). From $V'_{\infty,S}$ we determined g^*_S using Eqs. (16) and (13).

Given Q_1 and Q_2, g^*_L and g^*_S, given the velocity fields **U** derived from our flow fields around a cylinder, and given the velocity fields derived from our flow fields around a sphere, the trajectory of the drop and crystal was found by numerically integrating Eqs. (21) and (22) using a Hamming predictor-corrector-modifier method with the following initial conditions:

$$\left.\begin{aligned} V_{Lx_0} &= V'_{\infty,L}/V'_{\infty,L} = 1.0, & V_{Ly_0} &= 0 \\ V_{Sx_0} &= V'_{\infty,S}/V'_{\infty,L} = V_{\infty,S}, & V_{Sy_0} &= 0 \\ R_{Lx_0} &= R_{Sy_0} = 0, & R_{Sx_0} &= 100 \end{aligned}\right\}. \quad (27)$$

In computing those trajectories it was assumed that the circular cylindrical ice crystal falls with its c axis perpendicular to the direction of fall. Indeed, Jayaweera and Mason (1965) showed experimentally that this is the stable mode of fall of cylinders with $N_{\mathrm{Re},L} \leqslant 50$. In addition, it was assumed that Q_2 stayed constant during a particular trajectory. On the other hand, Q_1 was constantly updated in order to take into account the changing velocity of the drop as it approaches the crystal.

Our computations only pertain to the case where *columnar ice crystals collected drops*. Thus, our calculations were stopped when the free fallspeed of the droplet reached the free fall speed of the ice column. No computations were made for the case that water droplets collected ice crystals.

5. Numerical determination of the efficiency with which spherical water drops collide with circular cylindrical ice crystals of finite length

For a sphere interacting with another sphere, it has been customary to define the collision efficiency E by the relation $E=\pi(r'_c)^2/\pi(a'_L+a'_S)^2$. The quantity r'_c is the critical, horizontal distance by which the center of the smaller sphere is separated from the center line of the large sphere, as measured when the smaller sphere is far upstream, such that the smaller sphere makes grazing contract with the larger sphere while attempting to move around it. It has been customary to define the linear collision efficiency of two interacting spheres by $y_c=r'_c/a'_L$ so that, for interacting spheres $E=y_c^2/(1+p)^2$, where $p=a'_S/a'_L$. Obviously for a falling cylinder this definition cannot be used and E has to be defined in another manner. We have already justified in Section 2 that during the fall of a circular cylinder of finite length the velocity components along the cylindrical axis are negligibly affecting the trajectory of cloud drops. This implies that the efficiency with which a cloud drop collides with a cylindrical ice crystal of finite length is only negligibly affected by the position of the drop along the crystal's c axis but primarily depends on the distance of the drop from the axis of fall of the crystal in a plane perpendicular to the crystal's c axis. In recognition of this we shall define the collision efficiency of the crystal by

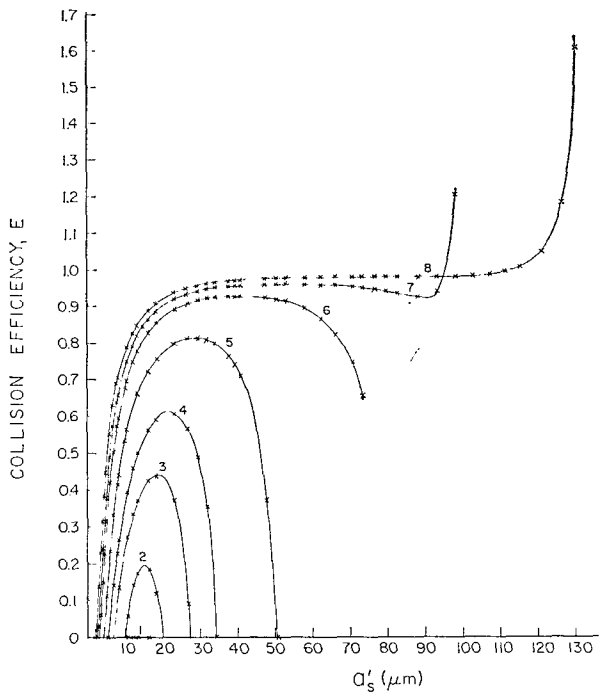

FIG. 3. Variation of the efficiency with which columnar ice crystals collide with water drops as a function of drop size:

1. $D'=$ 47.0 μm, $L'=$ 67.1 μm, $N_{\mathrm{Re},L}=0.2$;
2. $D'=$ 65.4 μm, $L'=$ 93.3 μm, $N_{\mathrm{Re},L}=0.5$;
3. $D'=$ 73.2 μm, $L'=112.6$ μm, $N_{\mathrm{Re},L}=0.7$;
4. $D'=$ 83.0 μm, $L'=138.3$ μm, $N_{\mathrm{Re},L}=1.0$;
5. $D'=106.8$ μm, $L'=237.4$ μm, $N_{\mathrm{Re},L}=2.0$;
6. $D'=154.4$ μm, $L'=514.9$ μm, $N_{\mathrm{Re},L}=5.0$;
7. $D'=213.4$ μm, $L'=1067$ μm, $N_{\mathrm{Re},L}=10$;
8. $D'=292.8$ μm, $L'=2440$ μm, $N_{\mathrm{Re},L}=20$.

$$E=r'_c/(a'_L+a'_S)=y_c/(1+p), \quad (28)$$

where $y_c=r'_c/a'_L$. By computing y_c from the critical trajectory on which a drop just made a grazing contact with the cylindrical ice crystal while falling with its c axis perpendicular to the fall direction, E was determined via Eq. (28). Values of E as a function of drop size, with the Reynolds number $N_{\mathrm{Re},L}$ of the crystal as a parameter, have been plotted in Fig. 3. In Fig. 4, E is plotted as a function of $V'_{\infty,S}/V'_{\infty,L}$ again with $N_{\mathrm{Re},L}$ as parameter.

It is seen from Figs. 3 and 4 that the collision efficiency increases with increasing drop size and increasing velocity ratio, to a broad maximum and subsequently tends to decrease to zero with further increase of these quantities. In the range $5 \leqslant N_{\mathrm{Re},L} < 10$ this tendency reverses such that, for $N_{\mathrm{Re},L} > 10$, E increases with increasing drop size and velocity ratio to a value larger than unity. The latter result is due to the effect of the

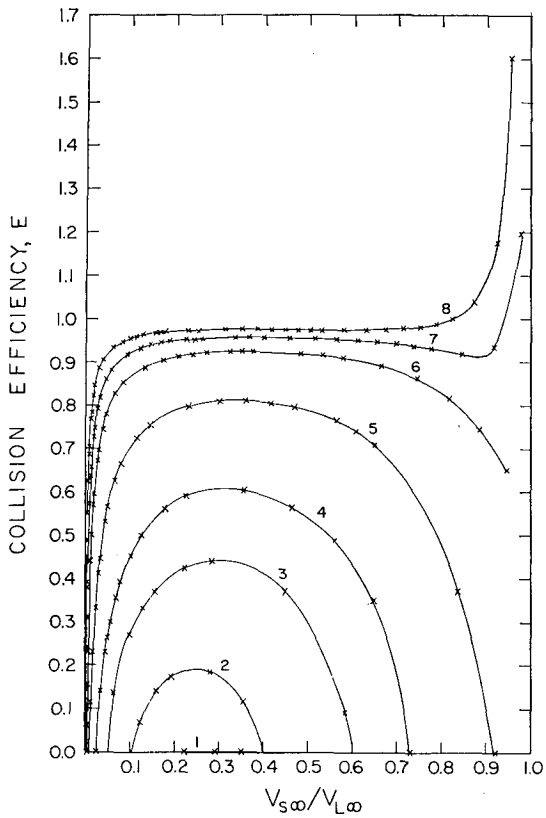

FIG. 4. Variation of the efficiency with which columnar ice crystals collide with water drops as a function of their terminal velocity ratio:

1. $D'=$ 47.0 μm, $L'=$ 67.1 μm, $N_{Re,L}=0.2$;
2. $D'=$ 65.4 μm, $L'=$ 93.3 μm, $N_{Re,L}=0.5$;
3. $D'=$ 73.2 μm, $L'=112.6$ μm, $N_{Re,L}=0.7$;
4. $D'=$ 83.0 μm, $L'=138.3$ μm, $N_{Re,L}=1.0$;
5. $D'=106.8$ μm, $L'=237.4$ μm, $N_{Re,L}=2.0$;
6. $D'=154.4$ μm, $L'=514.9$ μm, $N_{Re,L}=5.0$;
7. $D'=213.4$ μm, $L'=1067$ μm, $N_{Re,L}=10$;
8. $D'=292.8$ μm, $L'=2440$ μm, $N_{Re,L}=20$.

drop wake on the ice crystal. Another important conclusion which can be drawn from Figs. 3 and 4 is the fact that E decreases to zero for cylindrical ice crystals if their diameter is between 47.0 and 65.4 μm. This means that a columnar ice crystal has to grow to such a size by diffusion of water vapor before it can begin riming. This result is in excellent agreement with the observations of Iwai (1973), Ono (1969) and Hobbs (1971) who found from observation in atmospheric clouds that columnar ice crystals rarely are rimed if $D' \leqslant 50$ μm.

In conclusion it must be stressed that the collision efficiencies for thin plate-like ice crystals given by Pitter and Pruppacher (1974) and the presently computed collision efficiencies for columnar shaped ice crystals only apply to the very early stages of riming, i.e., as long as the shape of the crystal is still that of a thin plate or a column. As riming proceeds the ice particle changes shape and its collision efficiencies change. However, if one assumes that the riming leads to a spherical graupel particle some simple scheme may be devised which allows interpolation between the collision efficiency for the unrimed ice crystal and the collision efficiency for a sphere.

Acknowledgments. Two of the authors (R. J. Schlamp and H. R. Pruppacher) are indebted to the National Science Foundation for providing funds under Grants GA 32814X and DES 75-09999 which were used for carrying out a portion of the work reported in this article. One of the authors (A. E. Hamielec) is indebted to the Canadian National Research Council for providing funds needed to carry out some of the numerical computations reported in this article. Special thanks go to Dr. K. Iwai who provided us with several excellent photographs of rimed columnar ice crystals collected in atmospheric clouds. We further want to acknowledge the expertise of Mr. S. Grover who greatly helped us in setting up the numerical computations.

APPENDIX

Nomenclature

A	grid spacing in radial direction
AR	axis ratio of cylinder
a'_L	radius of cylindrical ice crystal
a'_S	radius of spherical drop
B	grid spacing in angular direction
C_D	total drag force coefficient for flow past an infinite cylinder
$C_{D,L}$	drag force coefficient of columnar ice crystal
$C_{D,S}$	drag force coefficient of drop
D'	diameter of cylindrical ice crystal
E	collision efficiency
$f'_{D,L}$	drag force on cylindrical ice crystal
$f'_{D,S}$	drag force on spherical water drop
g'	acceleration of gravity
I	polar angle index
J	radial coordinate index
$k(\theta)$	dimensionless pressure at surface of cylinder $\{=[p'(\theta)-p'_\infty]/\frac{1}{2}\rho'_a(V'_{\infty,L})^2\}$
$k(\theta=0)$	dimensionless frontal stagnation pressure at surface of cylinder $\{=[p'(\theta=0)-p'_\infty]/\frac{1}{2}\rho'_a(V'_{\infty,L})^2\}$
L'	length of cylindrical ice crystal
m'_L	mass of cylindrical ice crystal
m'_S	mass of spherical drop
p'	pressure
p	p-ratio $[=a'_S/a'_L]$
q	q-ratio $[=\rho'_L/\rho'_S]$
r'	radial coordinate
R_{Sx}, R_{Sy}	position coordinate of drop in Cartesian coordinate system
R_{Lx}, R_{Ly}	position coordinate of cylinder in Cartesian coordinate system
t'	time
U'_L	velocity of flow past cylindrical ice crystal

U_S' velocity of flow past spherical drop
V_L' instantaneous velocity of cylindrical ice crystal
V_S' instantaneous velocity of spherical drop
$V_{\infty,L}'$ terminal velocity of columnar ice crystal
$V_{\infty,S}'$ terminal velocity of drop
x vertical Cartesian coordinate
y horizontal Cartesian coordinate
y_c critical horizontal offset of drop from fall axis of cylinder such that drop makes grazing contact with cylinder
z defined by $r=r'/a_L'=e^z$.
ζ' vorticity of flow field around circular cylinder
ψ' streamfunction of flow field around circular cylinder
ρ_a' bulk density of air
$\rho_{L,S}'$ bulk density of ice crystal, bulk density of water drop
μ' dynamic viscosity of fluid
ν' kinematic viscosity of fluid
θ angular polar coordinate

REFERENCES

Auer, A. H., and D. L. Veal, 1970: The dimensions of ice crystals in natural clouds. *J. Atmos. Sci.*, **27**, 919–926.

Beard, K. V., 1974: Terminal velocity and deformation of raindrops aloft. *Preprints Conf. Cloud Phys.*, Tucson, Ariz., Amer. Meteor. Soc., 116–119.

Davies, C. N., and C. V. Peetz, 1956: Impingement of particles on a transverse cylinder. *Proc. Roy. Soc., London*, **A234**, 269–295.

Dennis, S. C. R., and G. Z. Chang, 1970: Numerical solutions for steady flow past a circular cylinder at Reynolds numbers up to 100. *J. Fluid Mech.*, **42**, 471–489.

——, and M. Shimshoni, 1964: The steady flow of a viscous fluid past a circular cylinder. Great Britain Astronaut. Res. Council, Current Papers, No. 797.

Griffin, F. O., 1972: The impaction of spherical particles on circular cylinders. M.S. thesis, Dept. Chem. Eng., University of British Columbia, Vancouver, Canada.

Hamielec, A. E., and J. D. Raal, 1969: Numerical studies of viscous flow around circular cylinders. *Phys. Fluids*, **12**, 11–17.

Hobbs, P. V., 1971: Studies of winter cyclonic storms over the Cascade Mountains. Research Rept. No. 6, Dept. Atmos. Sci., University of Washington, Seattle.

Homan, F., 1936: Einfluss grosser Zahigkeit bei Stromung um Zylinder. *Forschg. Geb. Ingenieurwes.*, **7**, 1-9.

Iwai, K., 1973: On the characteristic features of snow crystals developed along *c*-axis. *J. Meteor. Soc. Japan*, **51**, 458-466.

Jayaweera, K.O.L.F., and B. J. Mason, 1965: The behavior of freely falling cylinders and cones in a viscous fluid. *J. Fluid Mech.*, **22**, 709–720.

——, and R. E. Cottis, 1969: Fall velocities of plate-like and columnar ice crystals. *Quart. J. Roy. Meteor. Soc.*, **95**, 703–709.

Kajikawa, M., 1971: A model experimental study on the falling velocity of ice crystals. *J. Meteor. Soc., Japan*, **49**, 367–375.

Keller, H. B., and H. Takami, 1966: Numerical studies of steady viscous flow about cylinders. *Proc. Adv. Symp. Numerical Solutions of Nonlinear Differential Equations*, D. Greenspan, Ed., 9–11 May, University of Wisconsin, Madison, 115–140.

Klett, J., and M. H. Davis, 1973: Theoretical collision efficiencies of cloud droplets at small Reynolds numbers. *J. Atmos. Sci.*, **30**, 107–117.

LeClair, B. P., A. E. Hamielec and H. R. Pruppacher, 1970: A numerical study of the drag on a sphere at low and intermediate Reynolds numbers. *J. Atmos. Sci.*, **27**, 308–315.

Lin, C. L., and S. C. Lee, 1975: Collision efficiency of water drops in the atmosphere. *J. Atmos. Sci.* **32**, 1412–1418.

Mason, B. J., 1971: *The Physics of Clouds*, 2nd ed. Oxford University Press, 671 pp.

Neiburger, M., 1967: Collision efficiency of nearly equal size cloud drops. *Mon. Wea. Rev.*, **95**, 917–920.

Nieuwstadt, F., and H. B. Keller, 1973: Viscous flow past circular cylinder. *Comput. Fluids*, **1**, 59–71.

Nishioka, M., and H. Sato, 1974: Measurements of velocity distributions in the wake of a circular cylinder at low Reynolds numbers. *J. Fluid Mech.*, **65**, part 1, 97–112.

Ono, A., 1969: The shape and riming properties of ice crystals in natural clouds. *J. Atmos. Sci.*, **26**, 138–147.

Pitter, R. L., and H. R. Pruppacher, 1974: A numerical investigation of collision efficiencies of simple ice plates colliding with supercooled water drops. *J. Atmos. Sci.*, **31**, 551–559.

——, —— and A. E. Hamielec, 1973: A numerical study of the viscous flow past a thin oblate spheroid at low and intermediate Reynolds numbers. *J. Atmos. Sci.*, **30**, 125–134.

Pruppacher, H. R., B. P. LeClair and A. E. Hamielec, 1970: Some relations between drag and flow patterns of viscous flow past a sphere and a cylinder at low and intermediate Reynolds numbers. *J. Fluid. Mech.*, **44**, 781–790.

Ranz W. E., and J. B. Wong, 1952: Impaction of dust and smoke particles. *Ind. Eng. Chem.*, **44**, 1317–1380.

Shafrir, U., and M. Neiburger, 1963: Collision efficiencies of two spheres falling in a viscous medium. *J. Geophys. Res.*, **68**, 4141–4147.

——, and T. Gal-Chen, 1971: A numerical study of collision efficiencies and coalescence parameters for droplet pairs with radii up to 300 microns. *J. Atmos. Sci.*, **28**, 741–751.

Takami, H. and H. B. Keller, 1969: Steady two-dimensional viscous flow of an incompressible fluid past a circular cylinder-*Phys. Fluids*, **12**, Suppl. II, 51–56.

Taneda, S., 1956: Experimental investigation of the wakes behind cylinders and plates at low Reynolds numbers. *J. Phys. Soc. Japan*, **11**, 302–307.

Thom, H., 1933: The flow past circular cylinders at low speed. *Proc. Roy. Soc. London*, **A141**, 651–668.

Underwood, R. L., 1969: Calculation of incompressible flow past a circular cylinder at moderate Reynolds numbers. *J. Fluid Mech.*, **37**, 95–114.

Wilkins, R. I., and A. H. Auer, 1970: Riming properties of hexagonal ice crystals. *Preprints Conf. Cloud Phys.*, Fort Collins, Colo., Amer. Meteor. Soc., 81–82.

Woo, S., 1971: Simultaneous free and forced convection around submerged cylinders and spheres. Ph.D. thesis, McMaster University, Hamilton, Canada.

Woods, J. D., and B. J. Mason, 1965: The wake capture of drops in air. *Quart. J. Roy. Meteor. Soc.*, **91**, 35–43.

Zikmunda, J., and G. Vali, 1972: Fall patterns and fall velocities of rimed ice crystals. *J. Atmos. Sci.*, **29**, 1334–1347.